

Supplemental Data

Neurocalcin Delta Suppression Protects against Spinal Muscular Atrophy in Humans and across Species by Restoring Impaired Endocytosis

Markus Riessland, Anna Kaczmarek, Svenja Schneider, Kathryn J. Swoboda, Heiko Löhr, Cathleen Bradler, Vanessa Grysko, Maria Dimitriadi, Seyyedmohsen Hosseinibarkooie, Laura Torres-Benito, Miriam Peters, Aaradhita Upadhyay, Nasim Biglari, Sandra Kröber, Irmgard Hölker, Lutz Garbes, Christian Gilissen, Alexander Hoischen, Gudrun Nürnberg, Peter Nürnberg, Michael Walter, Frank Rigo, C. Frank Bennett, Min Jeong Kye, Anne C. Hart, Matthias Hammerschmidt, Peter Kloppenburg, and Brunhilde Wirth

SUPPLEMENTAL CASE REPORTS

Clinical Investigation of SMA Patients and Asymptomatic Family Members of the Utah Family.

Informed written consent (or parental consent and assent where appropriate) was obtained from all participating family members under University of Utah Institutional Review Board Protocol #8751 entitled Clinical and Genetics Studies in Spinal Muscular Atrophy. DNA was extracted from whole blood samples using routine protocols in all subjects; skin biopsies for fibroblast cultures were performed on a subset of individuals. All individuals with homozygous SMN deletion agreed to participate in additional detailed clinical investigations, including a full physical and neurological examination, electrophysiologic investigations inclusive of maximum ulnar compound muscle action potential amplitudes (CMAP) and motor unit number estimation (MUNE) to assess peripheral motor nerve function (using Vikingquest electromyography system, Natus and previously published protocol www.smaoutcomes.org, (Swoboda et al., 2005); dual energy X-ray absorptiometry (DEXA) scans to assess whole body composition and bone density (XR-26 system, Norland Corporation, Fort Atkinson, Wisconsin). A summary of phenotypes and investigations for *SMN1* deleted individuals is detailed below. History of evolution of clinical symptoms is additionally provided for the proband, 9164 and affected sister 9994 with SMA type I.

The proband was a female infant (**Figure 1A**, IV-2, SMA-I, 0 *SMN1*, 2 *SMN2* copies) born full-term following an uneventful pregnancy and delivery. In retrospect, parents noted hypotonia from about 2 weeks of age. Neurologic evaluation at age 3.8 months revealed generalized weakness and hypotonia, absent head control, areflexia and paradoxical breathing indicating intercostal muscle weakness. She had limited antigravity proximal limb movements. Ulnar CMAP was already significantly diminished: 0.9 mV (normal > 5 mV) and MUNE 8 (normal > 150). She received nocturnal noninvasive ventilatory support with bilevel respiratory support (BIPAP) from age 5.5 months. Nasogastric tube was required from 7 months and she received gastrostomy tube at 8.7 months. DEXA scan performed at 12 months of age revealed severely

diminished fat-free lean body mass for age. She died of respiratory failure at 3 years of age when her ventilator was inadvertently unplugged.

Unaffected brother (**Figure 1A**, IV-3, asymptomatic, 0 *SMN1*, 4 *SMN2* copies) was born full-term following an uneventful pregnancy, BW 6 lbs 14 oz. Prenatal diagnosis via amniocentesis was performed prior to the delivery. He was examined and followed closely prospectively from birth. Neurologic examination at 2 weeks, and 2, 3, 6, 9 and 12 months was normal. He sat by six months, stood by 9 months and walked independently by 10 months. CMAP was initially 3.8 mV at 2 weeks of age and progressively increased over the ensuing months, to reach a maximum of ~9 mV by 9 months of age. MUNE values were normal, and DEXA scan revealed normal body composition. He was evaluated on a yearly basis, and continued to develop normally. At 13 years of age, his neurologic exam is entirely normal; he can perform 20 squats without difficulty and he is normally active for age. He demonstrates a squint when going from dark to bright environments.

Unaffected brother (**Figure 1A**, IV-4, asymptomatic, 0 *SMN1*, 4 *SMN2* copies) was born full-term following an uneventful pregnancy and delivery, birth weight 8 lbs 2 oz. Examination at 1 day of age was normal. Detailed investigations performed at 3 months of age revealed normal CMAP (10.3 mV) and MUNE (~150) values. Developmental proceeded normally; he sat by 6 months and walked by 12 months. DEXA at 8 months demonstrated normal body composition. He demonstrated some modest speech delay, and was a bit clumsy but neurologic examination remained normal. At 11 years of age, he remains neurologically normal. He is normally active and can do 20 squats without evident difficulty or fatigue. He is photosensitive, with a prominent squint when going from dim to bright environment; this is especially notable in family photos taken outdoors.

Affected sister (**Figure 1A**, IV-5, SMA-I, 0 *SMN1*, 2 *SMN2*) was born 10 days post-term via induced vaginal delivery. At day 1 of life, she appeared clinically normal. However, by 4 days of age, she was hypotonic, with reduced spontaneous voluntary limb movements and evident tongue fasciculation. She was areflexic but still had good suck, cry and head control and

proximal antigravity limb movements. She had bilateral wrist drop and poor coloration of distal extremities. CMAP at 4 days of age was low (2.7 mV) and fell precipitously to 0.8 mV by 3 weeks of age, indicating rapidly progressive distal denervation. She received Nissan and gastrostomy-tube surgery at six weeks of age, and was on nocturnal BIPAP support by 3 months of age. She had numerous hospitalizations in the first year for acute on chronic respiratory failure, usually in the setting of apparent viral infections, including respiratory syncytial virus. She underwent tracheostomy at 22 months of age for increasing respiratory instability; however, support was withdrawn at 5 years of age after a critical illness with sepsis and multi-organ failure.

Unaffected father (**Figure 1A**, III-1, asymptomatic, 0 *SMN1*, 4 *SMN2* copies) underwent detailed clinical investigation at 30 years of age, when carrier testing indicated an apparent homozygous *SMN1* deletion. Detailed neurologic examination was entirely normal. Maximum ulnar CMAP (11.3 mV) and MUNE (150) values were normal. Whole body DEXA scan indicated normal body composition. He remains clinically unaffected at 43 years of age, without evidence of proximal muscle weakness or fatigability. He admits to photosensitivity, wears sunglasses most days, and has a characteristic squint in photos taken outdoors.

Unaffected paternal uncle (**Figure 1A**, III-4, asymptomatic, 0 *SMN1*, 4 *SMN2* copies) underwent detailed clinical investigation at 25 years of age. Detailed neurologic examination was normal, with no evident weakness or fatigability. Maximum ulnar CMAP (14.9 mV) and MUNE (160) values were normal. DEXA indicated normal body composition. At 37 years of age, he remains clinically asymptomatic. He was not examined for clinically evident photosensitivity.

Unaffected paternal aunt (**Figure 1A**, III-6, asymptomatic, 0 *SMN1*, 4 *SMN2* copies) underwent detailed clinical investigation at 22 years of age. Neurologic examination was normal, without evident weakness or fatigability. Maximum ulnar CMAP (10.6) and MUNE (160) values were normal. DEXA indicated normal body composition. At 35 years of age, she remains clinically asymptomatic. She was not examined for clinically evident photosensitivity.

SUPPLEMENTAL FIGURES AND LEGENDS

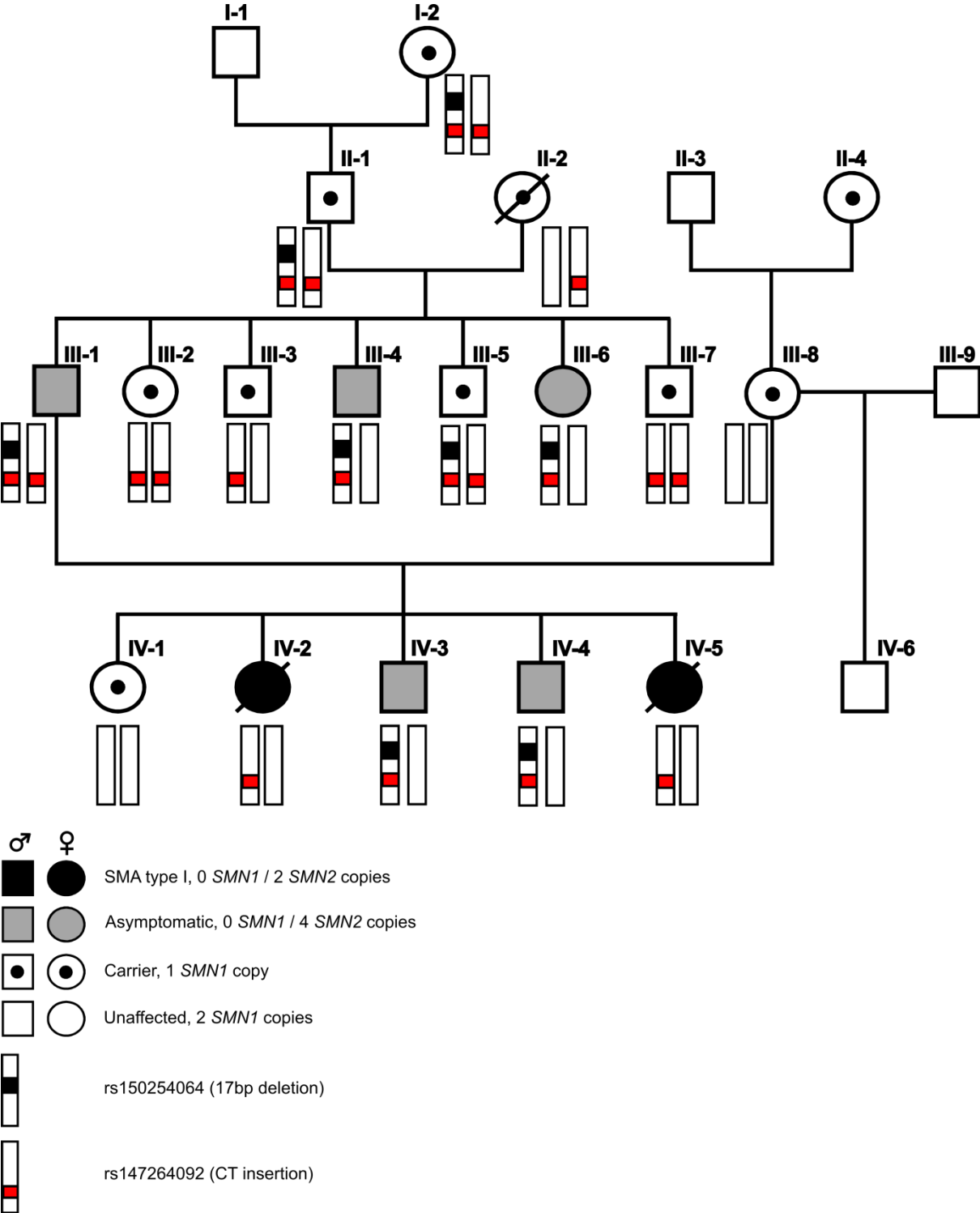


Figure S1 Pedigree showing of Utah family segregation of identified variants. (CT insertion in intron1 of *NCALD* and 17 bp deletion upstream of *NCALD*) on chromosome 8.

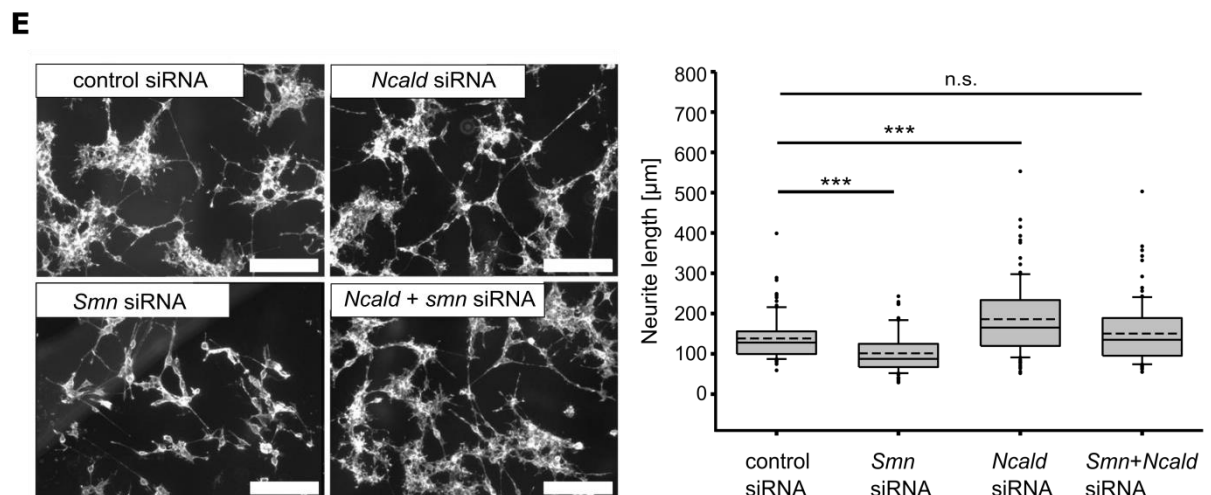
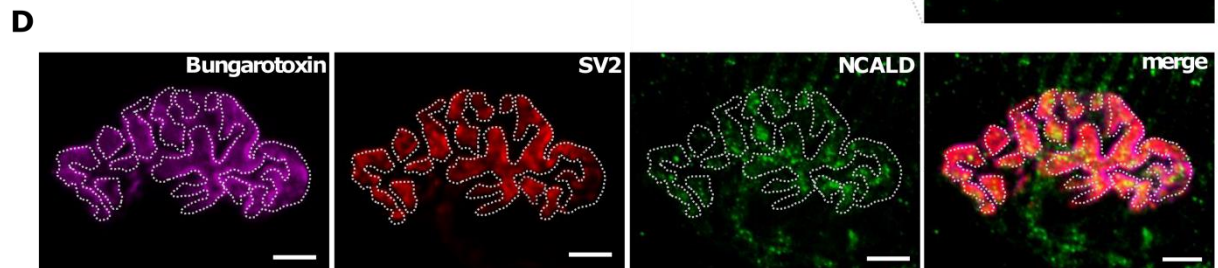
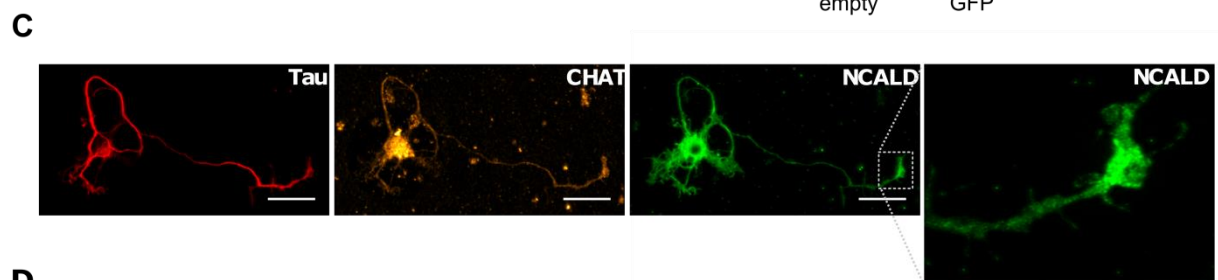
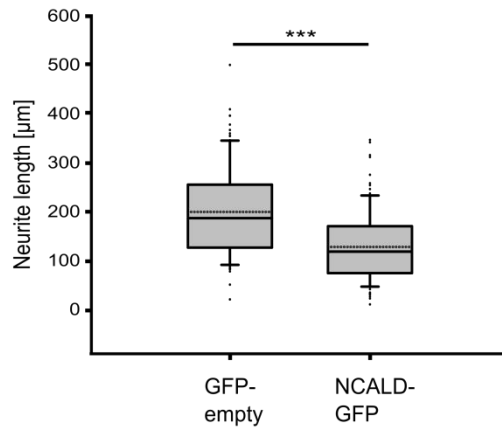
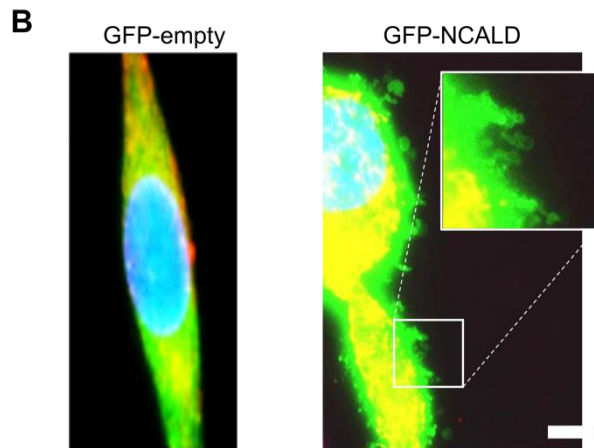
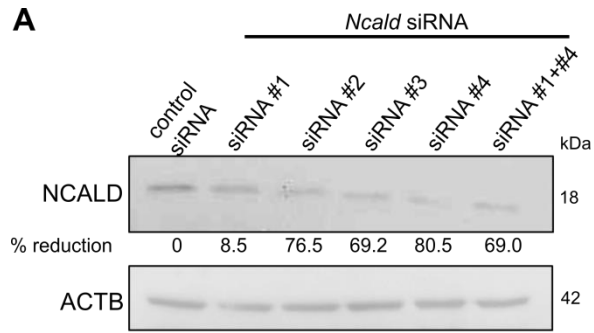


Figure S2. NCALD Downregulation Restores Neurite Outgrowth in SMN-Deficient Neuronal Cells, NCALD Overexpression Induces Membrane Blebbing.

(A) WB verifying NCALD reduction upon siRNA treatment 72h post transfection. 4 different siRNAs were tested; for all further experiments siNcald #2 was used. Numbers below NCALD blot indicate quantified percentage of knockdown efficiency.

(B) Representative image of an NSC34 cell overexpressing GFP or NCALD-GFP. Significant membrane blebbing is present only in the NCALD-GFP overexpressing cell. Inset shows detail of membrane blebbing. Scale bar, 10 μ m. Quantification of neurite outgrowth length of NSC34 cells transfected either with GFP or NCALD-GFP and treated with 1 μ m RA for 3 days and stained with Phalloidin-rhodamine. NCALD-GFP cells showed reduced neurite length. N = 100; ***P < 0.001.

(C) Representative images of primary murine MNs cultured 6 days *in vitro* (DIV) stained with antibodies against NCALD, Tau (axon-specific marker) and CHAT (MN-specific marker). Note the high expression of NCALD in soma and growth cones (inset). Scale bar, 50 μ m.

(D) Exemplary NCALD staining of NMJ in TVA of 3-week-old wt mice. Postsynaptic terminals stained with Bungarotoxin (magenta) and presynaptic terminals with SV2 (red, delineated by the dashed line). NCALD (green) localizes to presynaptic region, based on overlap between SV2 and NCALD, by Pearson's correlation of 0.72 ± 0.082 (Z stack, 0.5 μ m per stack; N = 4). Scale bar, 5 μ m.

(E) Representative images and quantification of neurite outgrowth of NSC34 cells treated with respective siRNAs (50nm) and differentiated with retinoic acid (1 μ M RA). 4 days after siRNA transfection and 3 days after RA treatment *Smn* siRNA cells showed neurite outgrowth defects. *Smn+Ncald* siRNA cells showed a phenotype rescue and an outgrowth comparable to control siRNA cells. Cells were stained with Phalloidin-Alexa Fluor 568. Scale bar, 200 μ m. N = 100 cells per treatment; ***P < 0.001; dashed line = mean (control siRNA: 138.32 μ m; *Smn* siRNA: 101.35 μ m; *Ncald* siRNA: 185.9 μ m; *Smn+Ncald* siRNA: 150.36 μ m), line=median (control siRNA: 122.5 μ m; *Smn* siRNA: 87.5 μ m; *Ncald* siRNA: 165 μ m; *Smn+Ncald* siRNA: 135 μ m).

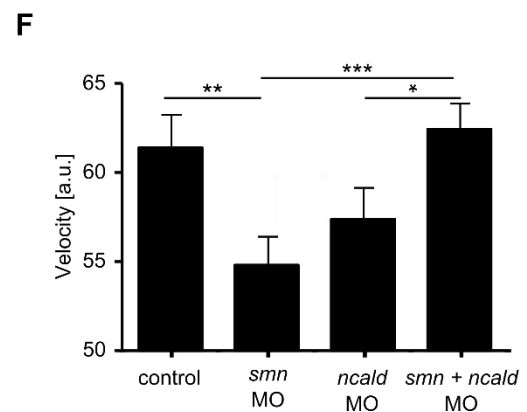
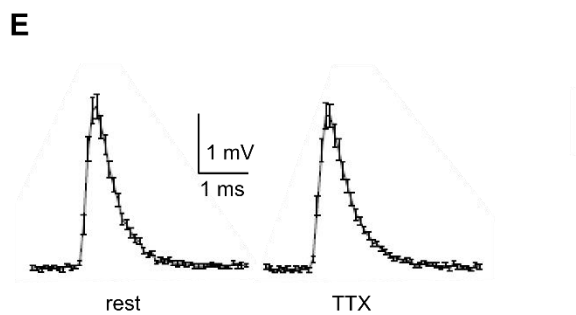
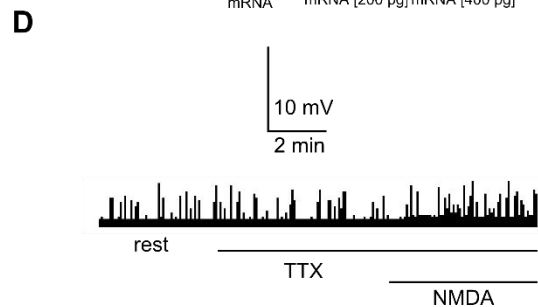
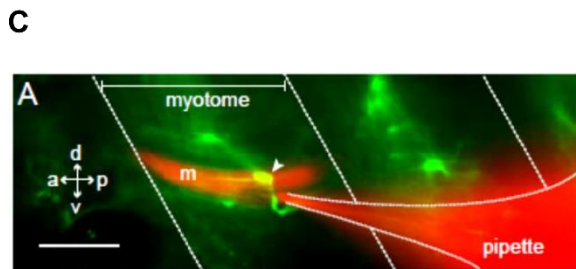
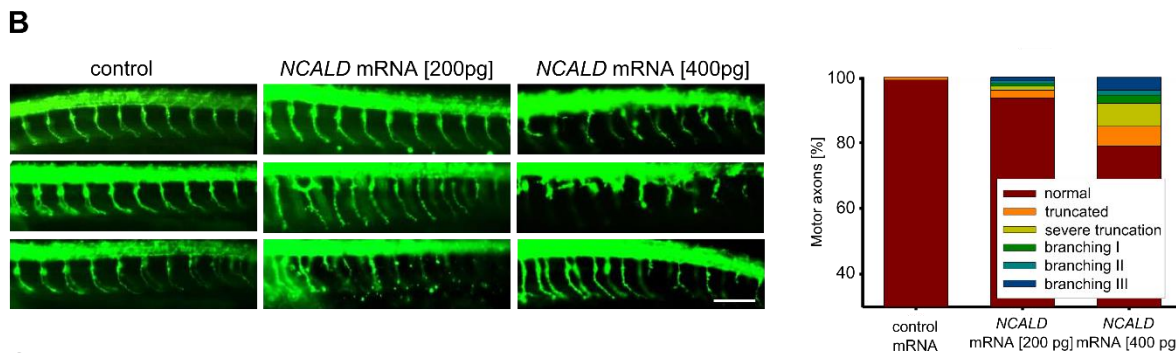
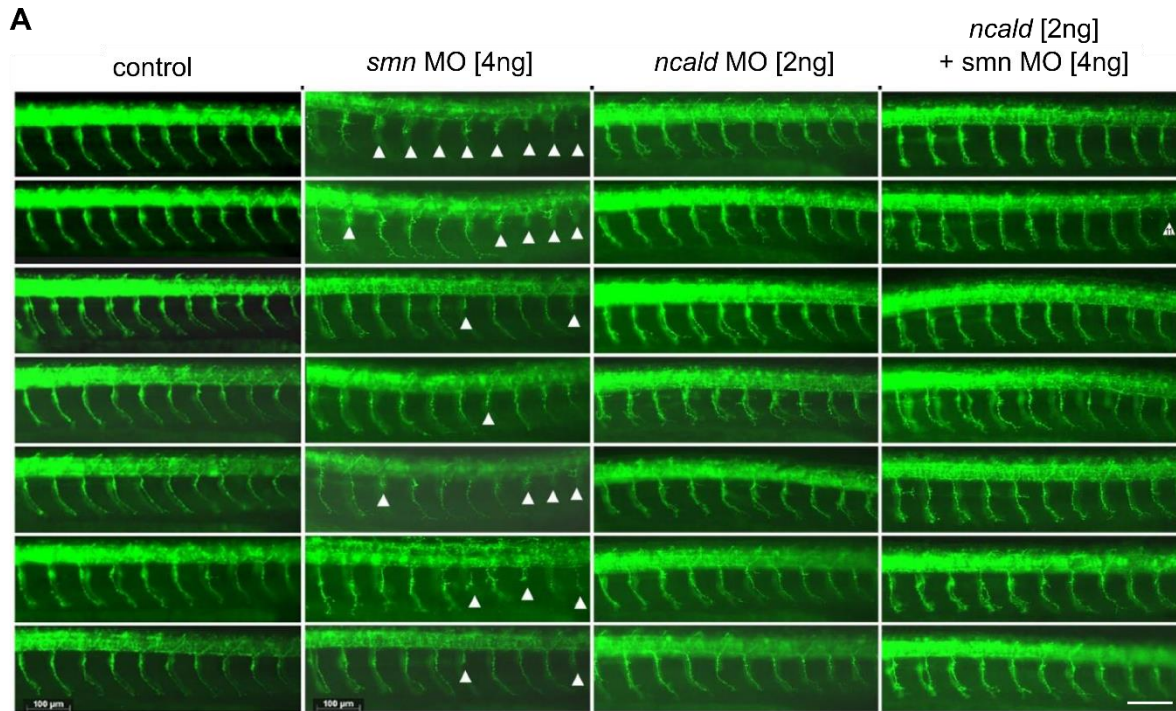


Figure S3. Overview of Motor Neuron Phenotype after Downregulation or Overexpression of NCALD and Characterization of Electrophysiological Properties of Zebrafish Muscles and Swimming Behavior of Zebrafish

(A) Representative overview of motor axon outgrowth phenotype of 34 hpf morphants (including pictures from main Figure 3). Significant truncation phenotype of *smn* morphants is corrected by additional *ncald* KD. Scale bar, 100 μ m.

(B) Representative overview of motor axon outgrowth phenotype of 34 hpf zebrafish after human *NCALD* mRNA injection. Quantification shows the dose-dependent truncation phenotype of zebrafish overexpressing *NCALD*. Scale bar, 100 μ m. First 10 motor axons posterior to the yolk were evaluated in every fish. $n \geq 200$ motor axons per mRNA injection.

(C) Fluorescence image of the recording situation. A wild-type ventral fast muscle cell was filled with rhodamine dextran (red) during a whole-cell patch-clamp recording. The muscle cell (m) is innervated by GFP-labeled motor neurons (green) indicated by the arrowhead. The muscle cell spans one myotome. Scale bar, 20 μ m.

(D) Whole-cell current clamp recordings of zebrafish muscles. Diagram shows original whole-cell current clamp recordings of mEPPs: at rest, during 1 μ M TTX, -and during simultaneous TTX- and 100 μ M NMDA-application. NMDA application failed to increase muscle action potentials in the presence of TTX. mEPP amplitude and frequency are not TTX-sensitive.

(E) Means of 30 EPPs in the absence or presence of 1 μ M TTX.

(F) Bar graph of high-speed camera swimming velocity measurement of 48 hpf zebrafish embryos (N = 30 per treatment). After LoLitracker software evaluation, mean swimming velocity is given in arbitrary units.

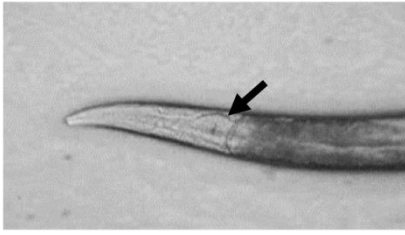
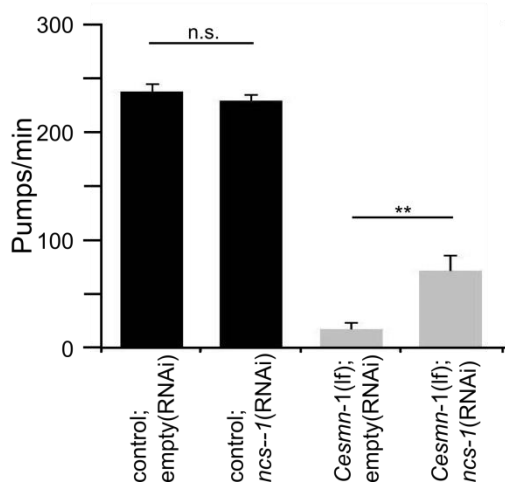
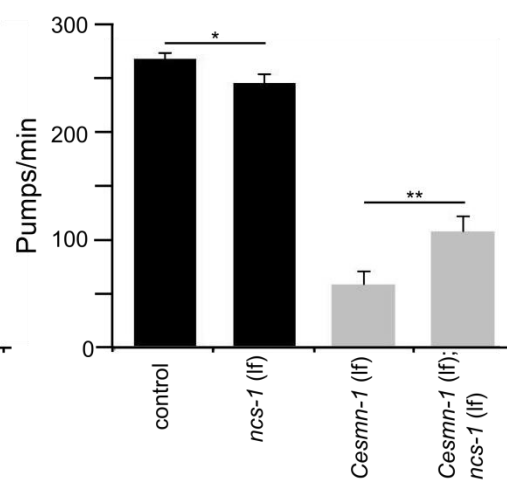
A**B****C**

Figure S4. *Nsc-1* (*ncald* Ortholog) Reduction Corrects the Phenotype in *C. elegans*

(A) *C. elegans* neuromuscular function was assessed based on pharyngeal pumping rates during feeding. Arrow indicates the pharyngeal grinder, which moves during each pumping event.

(B, C) Quantification of pharyngeal pumping in wild type or mutant *smn-1* worms fed with control or *ncs-1* RNAi knockdown (I) or with an *ncs-1*(*qa401*) mutant allele (J). For every determination $n \geq 25$. Mean \pm SEM is shown; * $P \leq 0.05$, ** $P \leq 0.01$.

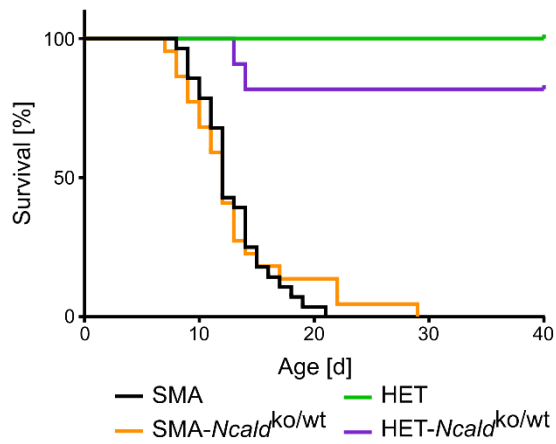
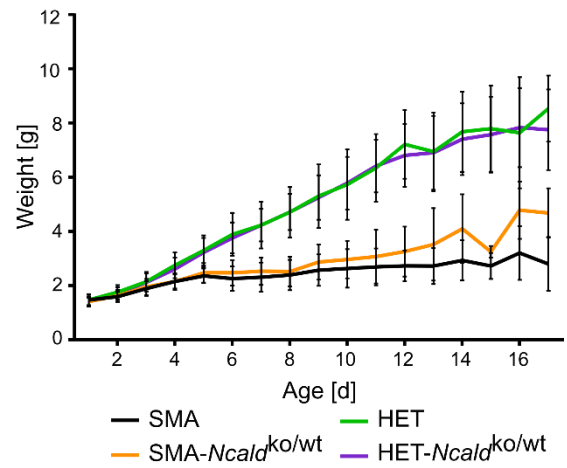
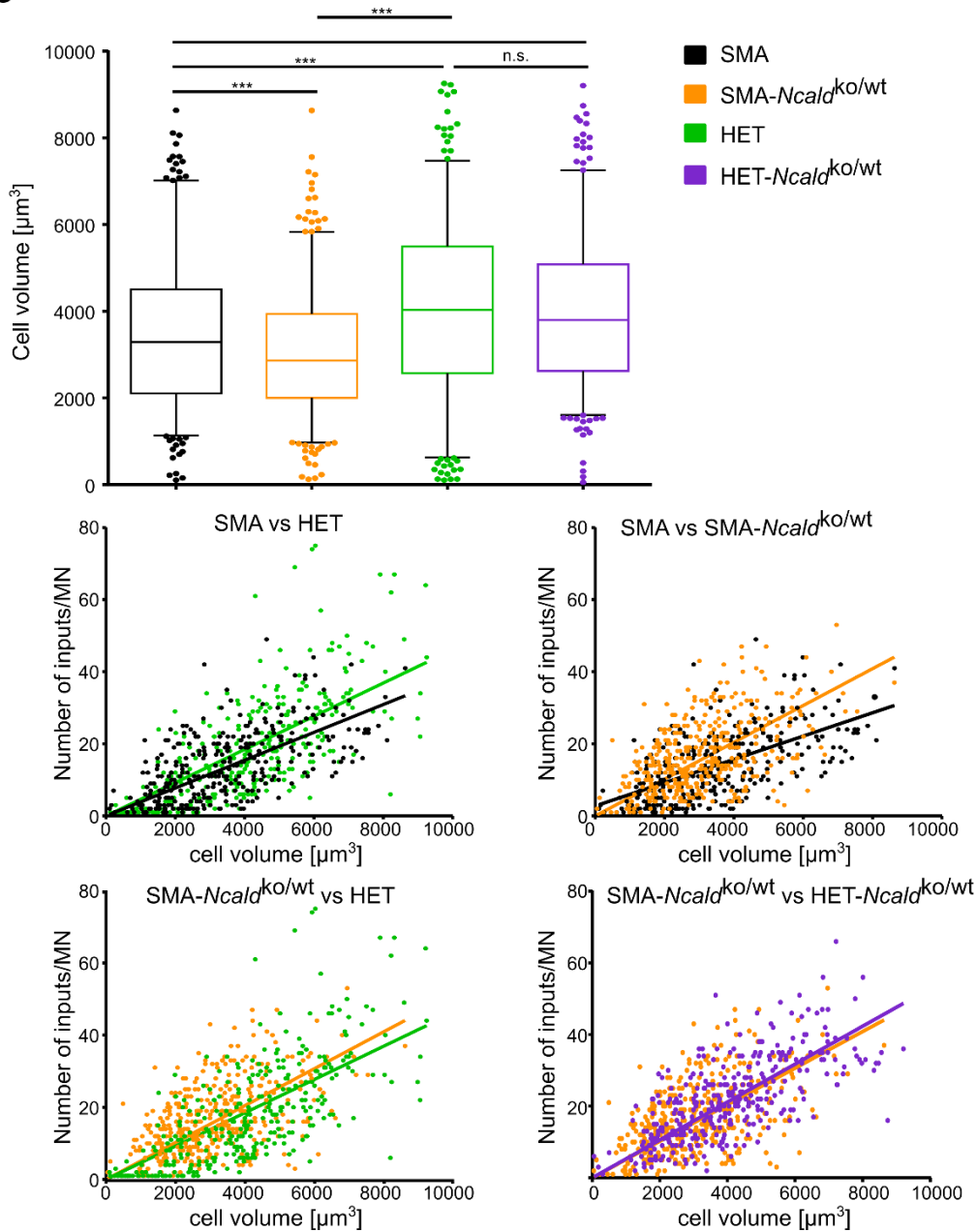
A**B****C**

Figure S5. Characterization of Heterozygous *Ncald* Knockout in SMA Mice: Survival, Weight Progression and Proprioceptive Inputs on Motor Neurons: Heterozygous *Ncald* Knockout Ameliorates Input Number but not Cell Size.

(A) Mean survival of SMA mice on pure C57BL/6N: SMA = 12.9 ± 3.2 days, N = 28, SMA-*Ncald*^{ko/wt} = 13.1 ± 5.3 days, N = 22.

(B) The weight of SMA and SMA-*Ncald*^{ko/wt} mice is reduced significantly from P5 onwards when compared to HET and HET-*Ncald*^{ko/wt}. Error bars indicate SD. N >20 for each genotype.

(C) The MN cell volume [μm^3] of SMA and SMA-*Ncald*^{ko/wt} is significantly smaller in comparison to HET. Analysis of proprioceptive inputs on spinal MN relative to cell volume: individual values of input number were plotted against cell volume and linear regression was drawn. The number of proprioceptive inputs in SMA-*Ncald*^{ko/wt} MN is increased independently of cell volume and input number/cell volume ratio was similar in SMA-*Ncald*^{ko/wt} and HET-*Ncald*^{ko/wt} MN. N = 3/genotype, n = 100-120 MN/animal. ***P < 0.001. Box plots defined in Figure 4.

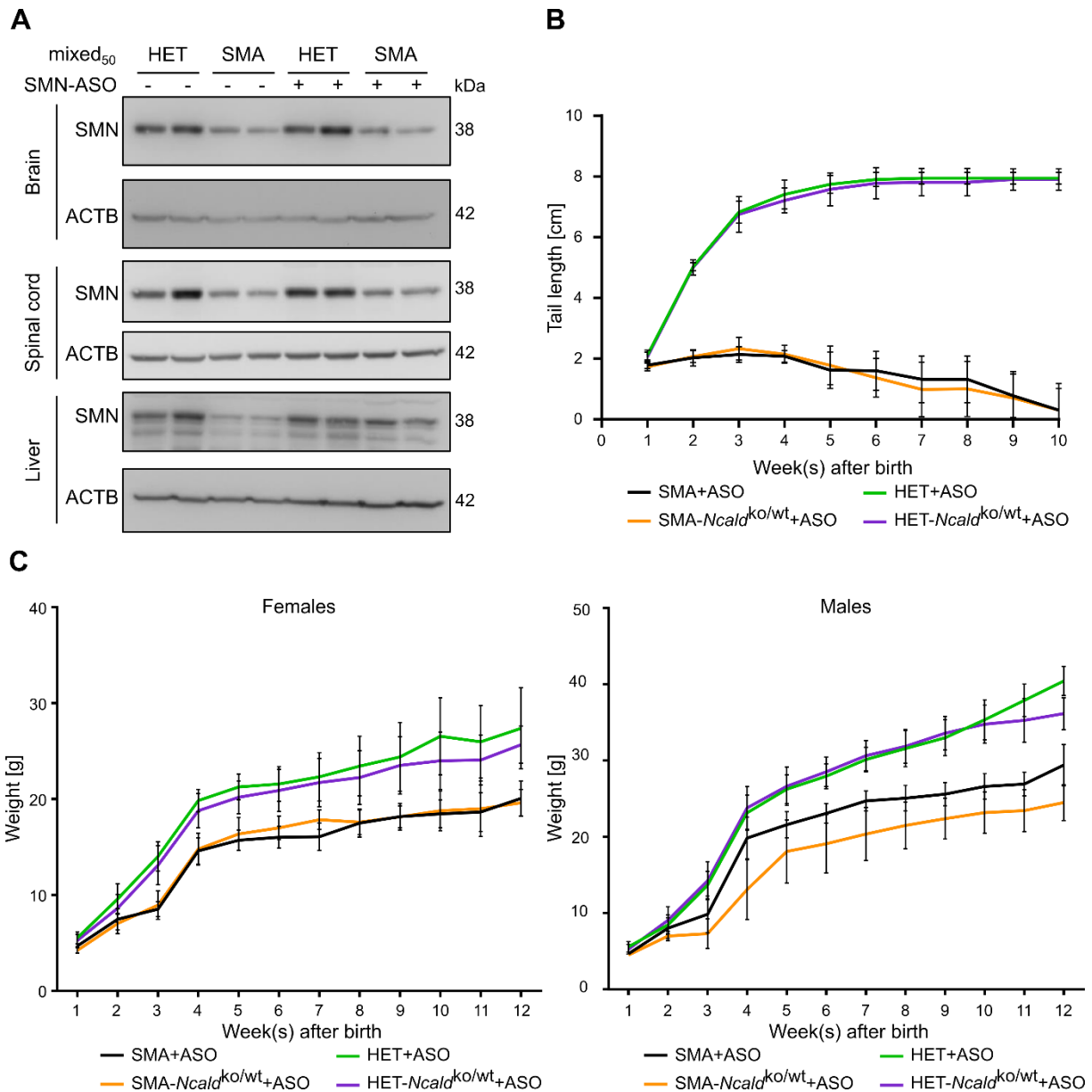


Figure S6 SMN-ASO Functionality Testing, Tail Length and Weight Progression in the SMA+ASO Mouse Model

(A) Western blot of spinal cord, brain and liver lysates of P4-old control-ASO or SMN-ASO injected mixed₅₀ HET or SMA mice. SMN levels were increased in the liver, but not in the brain or spinal cord after SMN-ASO injection. Beta-Actin (ACTB) was used as loading control.

(B) Tail length of SMN-ASO injected mixed₅₀ mice was measured weekly; tail necrosis in SMA+ASO (N = 7) and SMA-*Ncald*^{ko/wt}+ASO (N = 9) mice started between the 6th and 8th week after birth. Control mice: HET+ASO (N = 9); HET-*Ncald*^{ko/wt}+ASO (N = 10). Error bars indicate SD.

(C) Weight of female (F) and male (M) of SMN-ASO injected mixed₅₀ mice was measured weekly. SMA+ASO (F = 7, M = 5), SMA-*Ncald*^{ko/wt}+ASO (F = 4, M = 9), HET+ASO (F = 7, M = 9), HET-*Ncald*^{ko/wt}+ASO (F = 8, M = 9). Error bars indicate SD.

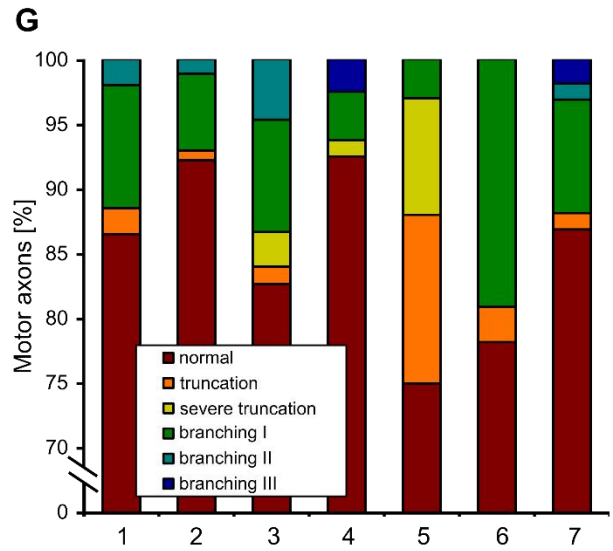
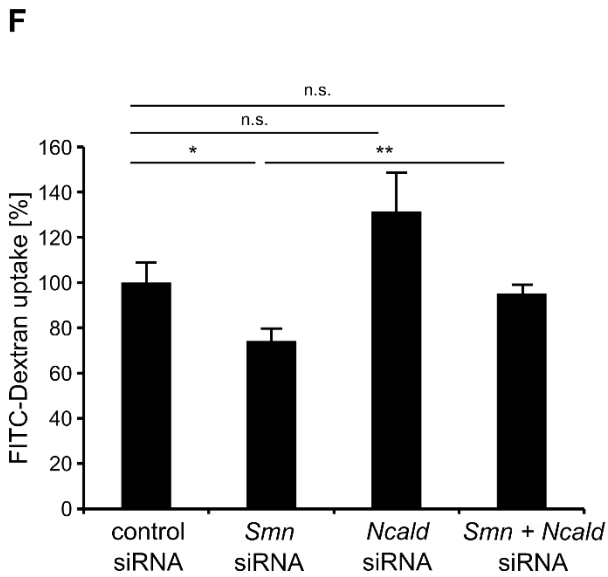
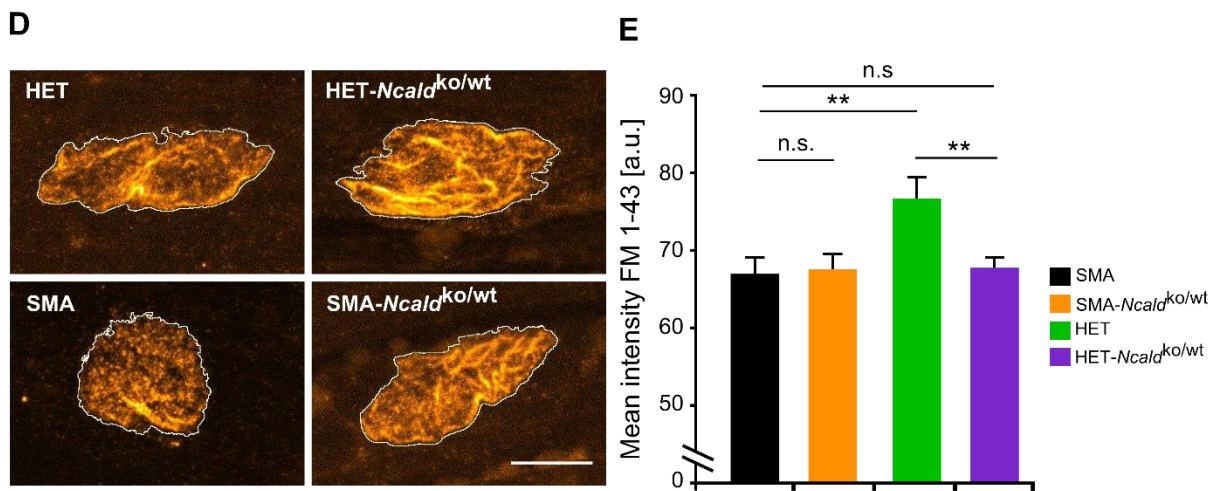
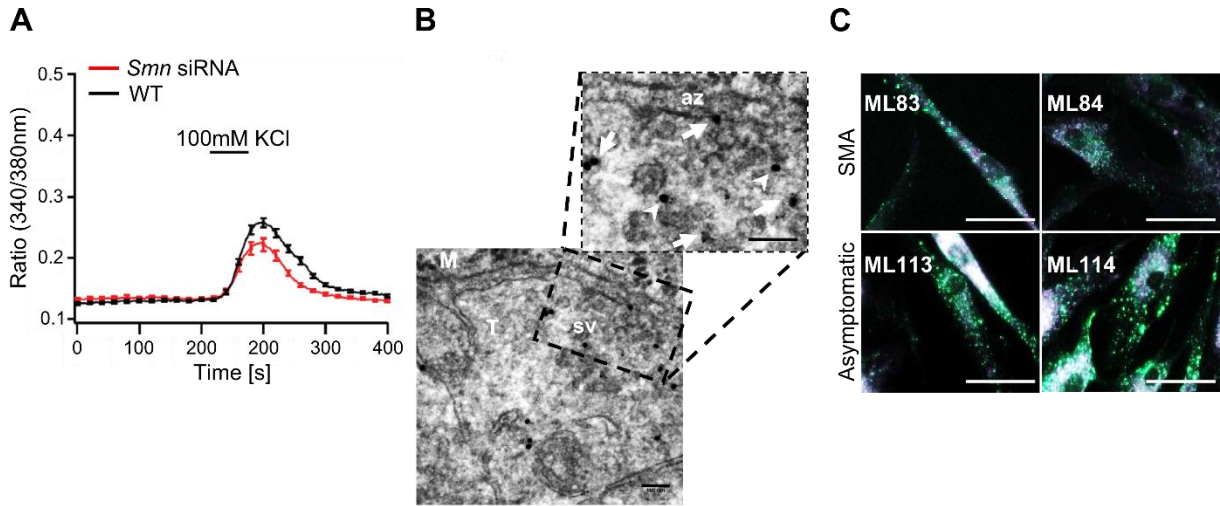


Figure S7 Voltage Induced Ca^{2+} Dynamics of Cells Treated with *Smn* siRNA or *Smn+Ncald* siRNA; Impact of Ca^{2+} on Endocytosis

(A) Ratiometric Ca^{2+} imaging with fura-2 in differentiated PC12 cells showed that the increase in cytosolic Ca^{2+} , which is triggered by KCl-induced, is reduced in SMN depleted cells (N = 3, n = 41) compared to control cells (N = 3, n = 38); $P < 0.001$.

(B) Immunogold staining of NMJs of 48 hpf control zebrafish embryos. *Ncald* is visualized by secondary antibody labelled with 20 nm gold particle (big black dots) and clathrin with 6 nm gold particle (small black dots). *Ncald* (white arrows) is localized to synaptic vesicles and the active zone (az) of the presynapse and clathrin is localized to some synaptic vesicles (black arrows); white arrowheads mark the colocalization of *Ncald* and clathrin at synaptic vesicles. M = muscle fiber, T = nerve terminal, scale bar, 100 nm.

(C) Representative images of fibroblasts derived from Utah family members, SMA patients and controls after endocytosis assay. After starvation cells were incubated for 20 min with FITC-dextran (green), fixed and counterstained with phalloidin-AlexaFluor 568 (red). The FITC signal is higher in asymptomatic cells. Scale bar, 50 μm . For quantification see also Figure 5C.

(D) Representative images of endocytic FM1-43 uptake at the presynaptic terminals on P10 in TVA muscles under low frequency stimulation (5 Hz, 1s). Postsynaptic receptors staining (BTX-Alexa647) was used to define the area to analyze the FM1-43 uptake (orange) at the presynaptic terminals. Scale bar, 10 μm . For quantification see also Figure 5D.

(E) Quantification of the FM1-43 mean intensity at the presynaptic terminals on P10 in TVA muscles under high frequency stimulation (20 Hz, 1s). For each genotype 3 animals and ~100 NMJs were analysed. Error bars represent SEM. n.s. non-significant; *** $P < 0.001$.

(F) FACS-based quantification of FITC signal in NSC34 cells treated with respective siRNA. *Ncald* KD resulted in elevated FITC-dextran endocytosis. *Smn* KD decreased endocytosis (* $P < 0.05$), which was fully restored by additional *Ncald* KD (*Smn* siRNA vs. *Smn+Ncald* siRNA: ** $P < 0.01$ control siRNA vs. *Smn+Ncald* siRNA: n.s.). N=6 biological replicates per siRNA treatment, individual sample n=50.000 cells.

(G) Quantitative analysis of motor axon phenotype of 34 hpf zebrafish, subjected to the respective treatment: 1 = *ncaId* MO (2 ng), 2 = *smn+ncaId* MO (2 ng), 3 = *ncaId* MO + Pitstop2 (12.5 μM), 4 = control + Pitstop2 (25 μM), 5 = *smn* MO + Pitstop2 (25 μM), 6 = *smn* MO+*ncaId* MO + Pitstop2 (25 μM), 7 = *ncaId* MO + Dynasore (25 μM). Note the rescue effect of *ncaId* MO injection on the truncation phenotype of *smn* MO and 25 μM Pitstop2 treated zebrafish (bars 5 and 6).

SUPPLEMENTAL TABLE

Table S1 Human fibroblast and EBV-transformed lymphoblastoid cell lines (LBs) derived from SMA patients, carriers and asymptomatic individuals used in this work.

Phenotype Utah Family	ID-No	SMN1/SMN2	DNA#	Fibroblast #	LB#
SMA type I	IV-5	0/2	9994	ML83	B9994
SMA type I	IV-2	0/2	9164	ML84	B9164
asymptomatic	IV-4	0/4	9120	ML113	B9120
asymptomatic	IV-3	0/4	9119	ML114	B9119
asymptomatic	III-1	0/4	9128	ML115	B9128
asymptomatic	III-4	0/4	9124	ML117	B9124
asymptomatic	III-6	0/4	9126	ML118	B9126
carrier	II-1	1/3	9129	ML146	B9129
carrier	III-2	1/1	9122		B9122
carrier	III-3	1/1	9123		B9123
carrier	III-5	1/4	9125		B9125
carrier	III-7	1/4	9127		B9127
carrier	I-2	1/4	9133		B9133
carrier	III-8	1/2	9165		B9165
carrier	IV-1	1/2	9118		B9118
carrier	II-4	1/2	9132		B9132
non-carrier	I-1	2/0	9134		B9134
Independent SMA patients					
SMA type III		0/3	326		BW70
SMA type II		0/4	798		BW174
SMA type II		0/4	1086		BW214
SMA type III		0/4	2349		BW303
SMA type III		0/4	1141		BW232
SMA type II		0/4	146		T110/91
SMA type III		0/4	906		BW184
SMA type III		0/4	106		T77/91
SMA type III		0/4	530		BW145
SMA type III		0/5	6241		LN498
SMA type III		0/4	6981f	ML69	
SMA type I		0/2	3413	ML17	
SMA type III		0/3	2027	ML12	BW332
SMA type I		0/3	4043	ML16	
SMA type III		0/3	2026	ML14	BW333
SMA type III		0/4	11268c	ML106	
SMA type II		0/3	785	ML5	
SMA type I		0/2	4814b	ML39	
control				ML32	
control				ML35	
control				ML44	

SUPPLEMENTAL REFERENCES

Swoboda, K.J., Prior, T.W., Scott, C.B., McNaught, T.P., Wride, M.C., Reyna, S.P., and Bromberg, M.B. (2005). Natural history of denervation in SMA: relation to age, SMN2 copy number, and function. *Ann Neurol* 57, 704-712.